

Separation of source, propagation and local site effects from accelerographs and its application to predict strong ground motion by summing small events

Masaru Tai & Yoshinori Iwasaki
 Geo-Research Institute, Osaka Soil Test Laboratory, Japan
 Minoru Oue
 The Kansai Electric Power Company, Japan

ABSTRACT: In this paper, we try to evaluate source effects, propagation path effects in connection with the geometrical attenuation and anelasticity (Q-value) as well as local site effects in frequency domain from S-wave of accelerographs observed at Kinki and Kanto districts. In this inversion we can get source parameter, Q_s -value, and site amplification factor in frequency domain. Then we compared the results by this inversion with the results of other workers by different theoretical method.

1 INTRODUCTION

Many statistical analysis of strong motion spectra have been carried out by many workers through out the world. Most of them were based on the multiple regression models in which the characteristics of the strong ground motion is assumed to vary linearly or logarithmic linearly according to the explanatory variables such as magnitude and epicentral distance, etc.

On the other hand, several authors (Papageogiou and Aki, 1983, Andrews, 1982, Iwata and Irikura, 1988) have tried to analyze observed seismograms to separate source, path, and local site effects. In this method, major controlling factors of observed seismograms have clearly physical meaning.

2 METHOD

We used the formulation of the inversion by Iwata and Irikura (1988). Spectral characteristic of observed S-wave motion at j-th site by i-th earthquake are considered to consist of three factors of source, path and local site effects as follows.

$$O_{ij}(f) = S_i(f) \cdot (1/R_{ij}) \exp(-\pi f R_{ij} / Q_s V_s) \cdot G_j(f) \quad (1)$$

where $O_{ij}(f)$; S-wave spectra at j-th site by i-th earthquake, $S_i(f)$; source spectra of i-th earthquake, Q_s ; quality factor of the crust along path, V_s ; average shear wave velocity along path, R_{ij} ; hypocentral distance. In order to obtain linear equations, Eq.(1) is modified by taking the logarithm. If seismic motions and these spectra were obtained at J stations by I earthquakes, we can construct $I \times J$ simultaneous equations. Then we solved resulting linear least square problem with inequality constraints where $G_j(f) \geq 1.0$ using the singular value decomposition method (Lawson and Hanson, 1974).

3 DATA SETS

Accelerographs that we used have been recorded by seismic network array station in Kanto district operating Strong Ground Observing Project of the Association of Electric Power Companies in Japan. Among the earthquake records from 1979 / 6 to 1983 / 6, we used two independent data sets according to two different regions. Data set1 (KANTO 1) is for earthquakes

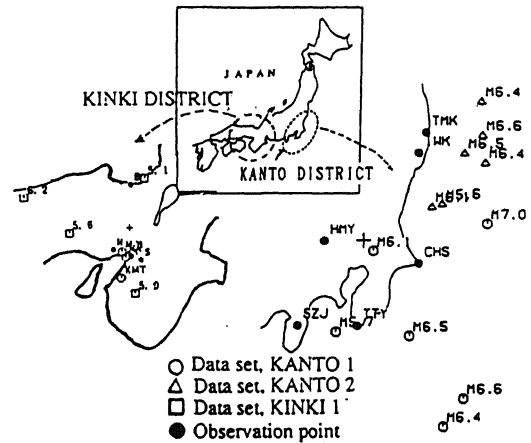


Figure 1. The map of the epicentral locations used in the inversion. (KANTO 1, 2, KINKI)

(M=5.7~7.0) occurred in the southern part and data set2 (KANTO 2) is for earthquakes (M=5.6~6.6) occurred in the northern part of Kanto District. Data set, KANTO1 is observed at 4 stations, SZY, TTY, HMY, CHS. Data set, KANTO 2 is observed at 3 stations, IWK, TMK, CHS. Only CHS is common to two data sets (KANTO 1, KANTO 2).

In Kinki District we used the accelerographs that observed at 4 stations, B, A, S, and R by the earthquakes (M=5.1~6.2) and this data set is KINKI. In Fig.1, we show the hypocentral locations by JMA and the stations in our study.

4 RESULTS OF THE INVERSION

4.1 Q_s -value as a function of frequency

Fig.2 (a) (b) shows the $1 / Q_s(f)$ obtained by the inversion as a function of frequency using data set, KANTO1, KANTO2, KINKI. All results of $1 / Q_s(f)$ clearly tend to decrease with frequency at high frequency domain. The frequency dependence of Q_s -value is roughly proportional to $(\text{frequency})^{-n}$ than 1.0 Hz. We find that in Kanto, n is 0.78 and in Kinki, n is 0.5. In Fig.2, we also plotted relations of $1 / Q_s$ -value and frequency obtained by

other method. The results in Kanto District are good agreement with the results of Aki (1979), Tsjuira (1978).

It is interesting that the relation of $1/Q_s(f)$ and frequency show the extreme values at low frequency domain and this result have been suggested by Aki (1979). The frequency of this extreme value may have important meaning. Assuming the crust is random medium, this frequency corresponds to the characteristic crack length (Yamashita, 1990, Matsumami, 1990, Sato, 1987). When we assumed the crust is random medium, we can use one dimensional scattering model for explaining the relation of $1/Q_s$ and f . (Sato, 1984). Fig.2 shows this theoretical relation of $1/Q_s$ and f by Sato (1984).

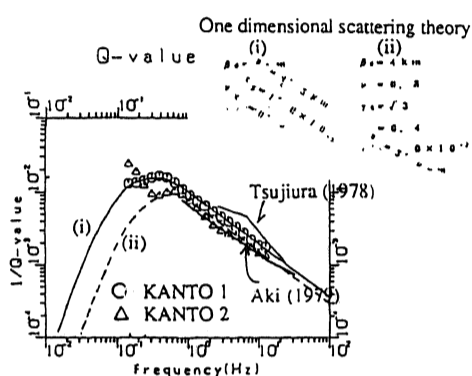


Figure 2. (a) Q_s -value by the inversion as a function of frequency. (KANTO 1, 2)

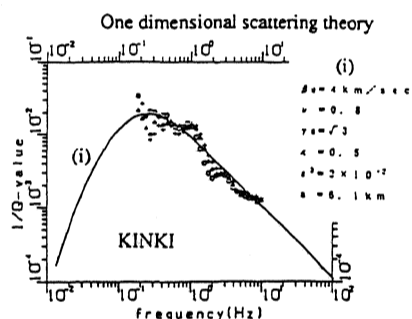


Figure 2. (b) Q_s -value by the inversion as a function of frequency. (KINKI)

4.2 Local site effects

Fig.3 (a) (b) shows the local site effects obtained from the data set, KANTO 1, KANTO 2 and KINKI. In data set, KANTO1, KANTO 2, site amplification of CHS station must be the same. Then we can set site effects of TMK equal 1.0, because seismograms of TMK is settled up at G.L. -950m and this rock have $V_s=2.8\text{km/sec}$. Putting local site effects of TMK is equal 1.0, the other site amplification effects are shown in Fig.3 (a). In Kinki District (data set, KINKI). We can set site effect of B equal 1.0, because seismograms of B station is settled up at the rock ($V_s=2.8\text{km/sec}$)

Table-1 shows the structure parameters (SZY, TTY, HMY, CHS) for the theoretical calculation using Hackell's method including the effects of inelastic attenuations. The results of theoretical calculation are shown in Fig.3 (a). The site effects by the inversion agree well with the theoretical amplification factors. Site S in Kinki district is outcropping hard rock site. ($V_s=1.4\text{km/sec}$), and site R is outcropping weathered rock site.

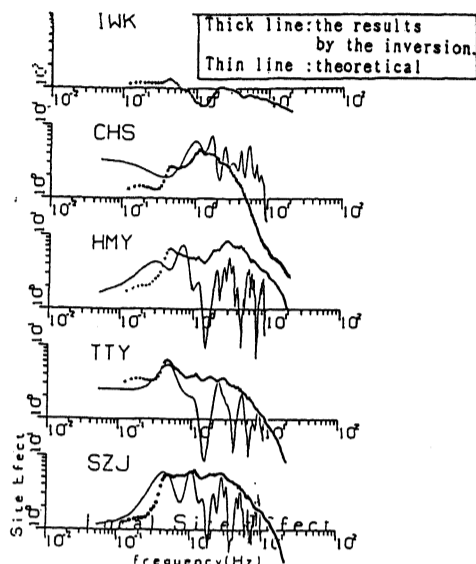


Figure 3. (a) The site amplification effects determined by the inversion, assuming that local site effects of TMK equal 1.0 and the theoretical amplification factor. (KANTO 1, 2)

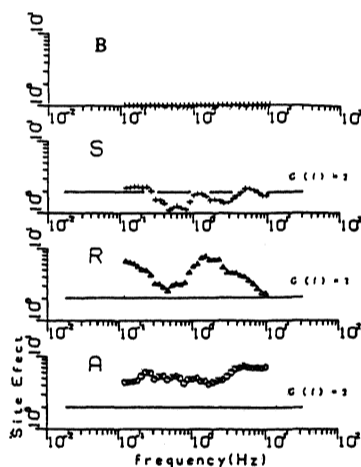


Figure 3. (b) The site amplification effects determined by the inversion (KINKI)

Table 1, structure parameters (KANTO 1, 2)

SZJ (Syuzenji)				TTY (Tateyama)			
1)	2)	3)	4)	1)	2)	3)	4)
1	1.4	150.	0.047	1	3.0	100.	0.000
2	5.6	300.	0.032	2	4.0	200.	0.021
3	4.6	300.	0.019	3	6.9	400.	0.013
4	6.9	690.	0.006	4	5.9	560.	0.008
5	3.9	220.	0.029	5	6.1	280.	0.021
6	7.3	500.	0.010	6	42.1	600.	0.008
7	1.9	160.	0.043	7	34.0	640.	0.007
8	7.3	650.	0.007	8	198.0	640.	0.007
9	4.4	280.	0.021	9	2000.0	1500.	0.002
10	6.7	850.	0.005	10	5000.0	2500.	0.001
11	5.6	330.	0.017	11	6200.0	3100.	0.001
12	3.4	690.	0.006	12	14000.0	3900.	0.001
13	2.0	400.	0.013				
14	10.0	650.	0.007				
15	2.1	150.	0.016				
16	6.0	650.	0.007				
17	4.0	850.	0.005				
18	4.6	600.	0.008				
19	5.4	800.	0.005				
20	4.9	700.	0.006				
21	200.0	700.	0.006				
22	700.0	1450.	0.002				
23	1000.0	2300.	0.001				
24	2000.0	2500.	0.001				
25	15000.0	3700.	0.001				
26	17000.0	3900.	0.001				

1) layer No.
2) thickness H(m)
3) S-wave velocity V_s (m/sec)
4) damping h
 $h=1/2Q$

Table 1. structure parameters (KANTO 1, 2)

HMY (Higashimatsuyama)				CHS (Chyoshi)			
1)	2)	3)	4)	1)	2)	3)	4)
1	1.9	300.	0.019	1	1.3	110.	0.070
2	10.6	650.	0.007	2	2.9	220.	0.029
3	9.7	1000.	0.004	3	2.0	330.	0.017
4	13.8	700.	0.006	4	2.2	540.	0.009
5	10.7	900.	0.005	5	0.9	450.	0.011
6	4.1	450.	0.011	6	2.9	1020.	0.004
7	27.6	750.	0.006	7	1.3	700.	0.006
8	5.9	600.	0.008	8	1.9	1050.	0.004
9	14.4	750.	0.006	9	2.6	1400.	0.003
10	5.9	650.	0.007	10	282.0	1400.	0.003
11	14.5	750.	0.006	11	100.0	2500.	0.001
12	179.0	750.	0.006	12	4500.0	3100.	0.001
13	1000.0	1500.	0.002	13	10600.0	3400.	0.001
14	4500.0	3000.	0.001	14	16900.0	3700.	0.001
15	10600.0	3400.	0.001				
16	16900.0	3700.	0.001				

4.3 Source spectra

Source displacement spectra obtained by the inversion are plotted in Fig.4 (a) (b) (c). In Fig.4, we find corner frequency to by using Andrews (1986) method. Source displacement spectra have flat level at low frequency and have f_0 and tend to decrease with frequency, being proportional to (frequency)⁻². These results show that source displacement spectra fit to ω^{-2} model.

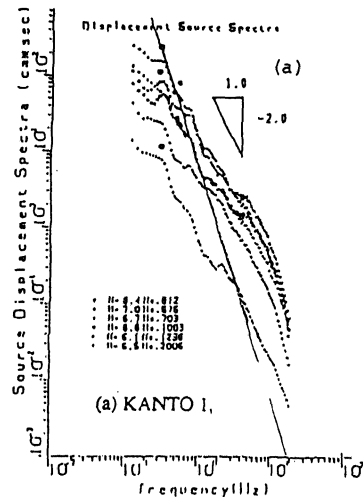


Figure 4. The source displacement amplitude spectra determined by the inversion. (a) KANTO 1

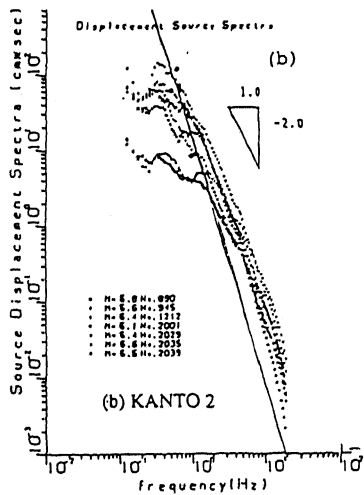


Figure 4. The source displacement amplitude spectra determined by the inversion. (b) KANTO 2

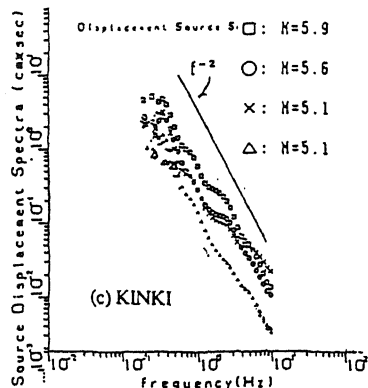


Figure 4. The source displacement amplitude spectra determined by the inversion. (c) KINKI

In the inversion, we can get propagation path effects, $\exp(-\pi f R_i / Q_s V_s) \cdot R_i$ and local site effects, $G_j(f)$ at each site. Then we shall determine source spectra using earthquake records by the equation as follows,

$$S_i(f) = [R_i \cdot \exp(-\pi f R_i / Q_s V_s) / G_j(f)] \cdot O_i(f) \quad (2)$$

Then we determined source spectra by Eq.(2). Specially we determined seismic moment M_0 , fault area S and stress drop $\Delta\sigma$ as follows.

$$M_0 = 4 \pi \rho V_s^3 R_0 / R_\phi \cdot \Omega_0$$

$$S = \pi r^2 = \rho (0.28 V_s / f_0)^2$$

$$\Delta\sigma = (7 / 16) M_0 / r^3$$

where ρ ; density = 2.7g / cm³ ; r_0 ; hypocentral distance,

R_ϕ ; radiation pattern=0.63, V_s ; shear wave velocity = 3.7km/sec,

Ω_0 ; the flat level of source displacement spectra at low frequency,

S ; fault area, r ; fault radius. f_0 ; corner frequency. $\Delta\sigma$; stress drop, M_0 ; seismic moment.

Fig.5 shows the relation of M_0 and f_0 is Kanto District. Fig.6 shows the distribution of stress drop in Kanto District. As the same, Fig.7, 8 is is Kinki District. Seismic moment M_0 is proportional to (corner frequency)⁻³ with some band width in both Kanto and Kinki District. Then we shall conclude that source

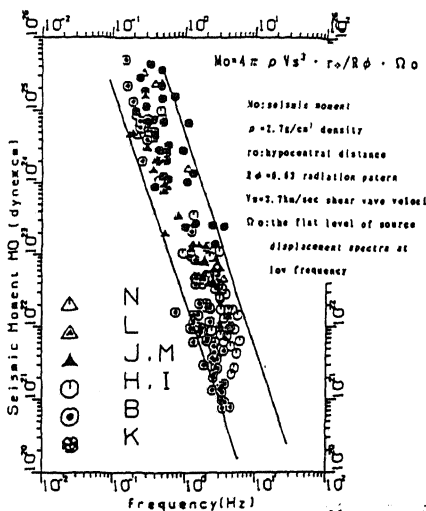


Figure 5. The logarithm of seismic moment M_0 versus the logarithm of corner frequency f_0 . (Kanto District) (Symbols of N, L, J, M, H, I, B, K are shown in Figure 6.)

displacement spectra fit to ω^{-2} model in magnitude range 3.9 ~ 7.0. But distribution of stress drop is different at the earthquake regions.

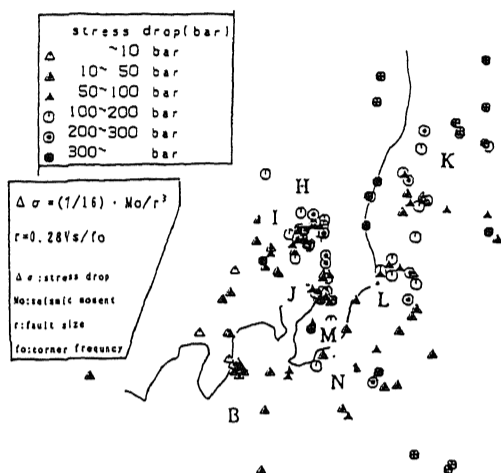


Figure 6. The distribution of static stress drop. (Kanto District)

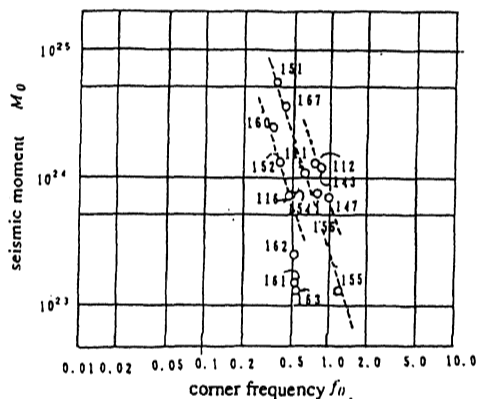


Figure 7. The logarithm of seismic moment M_0 versus the logarithm of corner frequency f_0 . (Number in this figure is shown in Figure. 8.) (Kinki District)

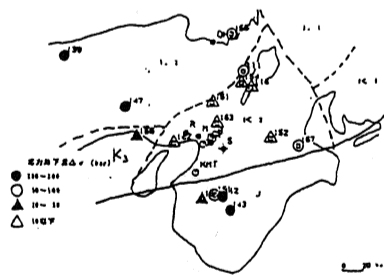


Figure 8. The distribution of static stress drop (Kinki District)

5 CONCLUSION

In recent years, earthquake records were observed by seismic net work array system at many regions. Our inversion method based upon multi-array data in a local region is very efficient to evaluate source effects, propagation path effects and local site effects using

earthquake records of these seismic array system. The three major controlling factors separated by this inversion are good agreement with the results of other workers by different theoretical methods.

1. Quality factor Q_s of the crust depends on frequency at the relation $Q_s \sim f^n$ ($n = 0.73$ in Kanto, $n = 1.0$ in Kinki District, frequency $\geq 1.0 Hz$). This relation is explained by one dimensional scattering model by Sato, 1984.

2. Local site effects nearly depend on the velocity and damping structures of the the layers at the site.

3. Source spectra fit to ω^{-2} models. But stress drop is different at the earthquake regions.

4. The results of separation show that we must consider the locality of site, path and source when we predict strong ground motion by summing observed small events at the site (Irikura, 1983, 1986)

6 ACKNOWLEDEMENT

The seismic records used in this paper were obtained by the joint research study on electric power companies in Japan, entitled "Study on the characteristics of seismic wave".

REFERENCE

- Andrews, D.J. (1982): Separation of source and propagation spectra of seven Mammoth Lakes aftershocks, Proceeding of workshop, Dynamic characteristic of faulting, U.S. Geol. Sur., Open File Rep., 437.
- Iwata, T. and Irikura, K. (1988): Source parameters of the 1983 Japan Sea Earthquake Sequence, J. Phys. Earth, 36.
- Aki, K. (1967): Scaling relation of seismic spectrum, J. Geophys. Res., 72.
- Papageorgiou, A.S. and Aki, K. (1983): A specific barrier model for the quantities description on in homogenous faulting and the prediction of strong ground motion, Bull. Seis. Soc. Am., 73.
- Sato, H. and Matsumura, S. (1980): Tree dimensional analysis of scattered P waves on the basic of the PP single isotropic scattering model, J. Phys. Earth, 28.
- Aki, K. (1980): Attenuation of shear waves in the lithosphere for frequencies from 0.05 to 25 Hz, Phys. Earth Planet, 21.
- Tsujiura, M. (1978): Spectral analysis of the coda waves from local earthquakes, Bull. Earthquake Res. Inst., Univ. Tokyo, 21.
- Lawson, C.L. and Hanson, R.J. (1974): Solving least squares problem, Prentice-Hall.
- Dobry, R., Idriss, I.M. and Ng, E. (1978): Duration characteristics of horizontal components of strong-motion earthquake record, Bull. Seis. Soc. Am., 68.
- Anderberg, M.R. (1973): Cluster analysis for applications, Academic Press, Inc.
- Yamashita, T. (1990): Attenuation and dispersion of SH waves due to scattering by randomly distributed cracks, PAGEOPH, 32, No.3.
- Matsunami, K. (1990): Laboratory measurements of spatial fluctuation and attenuation of elastic waves by scattering due to random heterogeneities, PAGEOPH.
- Andrews, D. J. (1986): Objective determination of source parameters and similarity of earthquakes of different size, in Earthquake Source Mechanics, Maurice Ewing Series 6.
- Irikura (1983): Semi-empirical estimation of strong ground motions during large earthquakes, Bull. Disaster Prevention Res. Inst., Kyoto Univ.
- Irikura, K. (1986): Prediction of strong acceleration motions using empirical greens function, Proc. of 7th Japan Earthquake Engineering Symp., Dec., 1986, Tokyo.